



Atomistic properties of helium in hcp titanium: A first-principles study

Yong-li Wang^a, Shi Liu^{a,*}, Li-jian Rong^a, Yuan-ming Wang^b

^aMaterials for Special Environment Department, Institute of Metal Research, Chinese Academy of Sciences, 72 Wenhua Road, Shenyang 110016, People's Republic of China

^bShenyang National Laboratory for Materials Science, Institute of Metal Research, Chinese Academy of Sciences, 72 Wenhua Road, Shenyang 110016, People's Republic of China

ARTICLE INFO

Article history:

Received 11 June 2009

Accepted 21 April 2010

ABSTRACT

First-principles calculations based on density functional theory have been performed to investigate the behaviors of He in hcp-type Ti. The most favorable interstitial site for He is not an ordinary octahedral or tetrahedral site, but a novel interstitial site (called FC) with a formation energy as low as 2.67 eV, locating the center of the face shared by two adjacent octahedrons. The origin was further analyzed by composition of formation energy of interstitial He defects and charge density of defect-free hcp Ti. It has also been found that an interstitial He atom can easily migrate along $\langle 001 \rangle$ direction with an activation energy of 0.34 eV and be trapped by another interstitial He atom with a high binding energy of 0.66 eV. In addition, the small He clusters with/without Ti vacancy have been compared in details and the formation energies of He_nV clusters with a pre-existing Ti vacancy are even higher than those of He_n clusters until $n \geq 3$.

© 2010 Elsevier B.V. All rights reserved.

1. Introduction

Helium is usually generated in tritium storage and in fission and future fusion reactors. It is normally insoluble in metals or metals tritides due to its inert reactivity with other elements, thereby precipitating as high-inner-pressured bubbles [1–10] that is responsible for the degradation of material properties and the shortening of lifetime for nuclear reactor components. Therefore, to study mechanism of trapping He and to learn its behaviors in metals make significant sense to nuclear industry.

During the past several decades, lots of theoretical simulations have been performed to reveal the atomistic properties of helium in metals, such as solution sites, migration mechanisms and barriers. Those build the first crucial step forward understanding mechanism of nucleation and growth associated with helium bubbles. In particular, the majority of calculations based on empirical potentials (EPs) [11–20] or density functional theory (DFT) [21–26] was performed for He only in both fcc and bcc metals. Theoretical study on He in hcp Ti has not been reported yet with respect to many experimental studies done [5,9,27–30].

Here, through first-principles calculations we reported He's behavior in hcp-type Ti by focusing on solution sites, migration barriers of interstitial He, and the stability of small helium or helium-vacancy clusters.

2. Computational details

The present calculations were performed using the plane-wave ultra-soft pseudopotential (PW-USPP) [31] method based on density functional theory (DFT). The PW91 form [32] of generalized gradient approximation (GGA) was applied as the exchange–correlation potential. The supercell approach with periodic boundary conditions was used to study defect properties as well as pure Ti systems. The supercells of Ti with or without defects (He atoms or vacancy) were optimized using the Broyden–Fletcher–Goldfarb–Shanno (BFGS) [33] algorithm by allowing both atomic positions and the lattice parameters to relax. During optimizations, the self-consistent loop terminated until the total energy was converged to 10^{-6} eV/atom and the force on each unconstrained atom less than 0.3 eV/nm, stress lower than 0.05 GPa and displacement smaller than 0.0001 nm. The supercells of 36 and 48 Ti atoms were adopted to investigate the effects of the supercell size on the properties of the dissolved He. The effects of cut-off energy were checked by applying 450 and 550 eV for the calculation for He dissolved in Ti, and the k-point grid spacing for the Brillouin zone integration was about 0.5 nm^{-1} .

The defect formation energy is defined as:

$$E_f = E_{m\text{Ti},n\text{He}} - mE_{\text{Ti}} - nE_{\text{He}}, \quad (1)$$

where $E_{m\text{Ti},n\text{He}}$ is the total energy of an optimized supercell containing $m\text{Ti}$ atoms and $n\text{He}$ atom, E_{Ti} is the energy per Ti atom in optimized hcp crystal, and E_{He} is the energy of an isolated He atom.

* Corresponding author.

E-mail address: sliu@imr.ac.cn (S. Liu).

2.1. Solution of He in hcp Ti

Fig. 1 shows various helium solution sites in the hcp-type Ti lattice, including substitutional (Sub), tetrahedral (TC), octahedral (OC), and FC (the center of equilateral trigonal face shared by two adjacent octahedrons) sites. To elaborate on the effects of the cut-off energy (E_{cut}) and the supercell size on the relative stabilities of He atom in those sites, their formation energies were further derived under three different options as shown in Table 1. It has been found that formation energy is insensitive to the choice of parameters. The formation energy for each solution site in the 36-atom supercell slightly increases only 0.01 eV as the E_{cut} changes from 450 to 550 eV, and the energy difference for each site is less than 0.03 eV between the 36 and 48-atom supercells. The relative values of formation energies for different sites vary as small as 0.01 eV for different options. These results show that the calculations with a cut-off energy 450 eV within the 36-atom supercell could qualitatively describe the relative stabilities of He atom in hcp Ti lattice, and the results discussed below are all obtained on the basis of this option.

In Table 1, the remarkable point is that the favorable site in energy for interstitial He atom is the FC site, rather than the maximum-spaced octahedral site. This FC preferential site is hardly reported before. The reason for this phenomenon will be discussed in next section. This result also challenges an intuitional consensus that small impurity atoms always tend to stay in the maximum-spaced interstitial sites [23]. Factually, similar results based on DFT have been reported that He atom in tetrahedral site is more stable than in the maximum-spaced octahedral one in the bcc Fe and other bcc metals [21–24], contradicting with the results based on EPS by Wilson [12]. Indeed, the latter was obtained within the empirical potentials. To crosscheck whether this unusual result for Ti is induced by the theoretical method used in present calculation, the relative stabilities of interstitial He in bcc Fe were calculated using the same method within a 54-atom Fe supercell. The results show that the formation energy of He in tetrahedral site

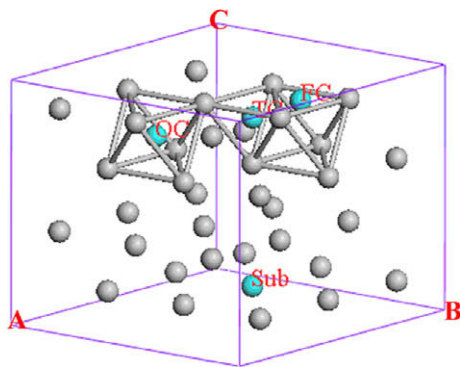


Fig. 1. The light blue ball represent the substitutional, tetrahedral (TC), octahedral (OC), and FC (the center of equilateral trigonal face of octahedron) sites. (For interpretation of the references to colour in this figure legend, the reader is referred to the web version of this article.)

Table 1
Formation energies (electron volts, eV) of He in various solution sites in hcp Ti.

	E_{cut}	E_f^{sub}	$E_f^{\text{(°C)}}$	E_f^{TC}	E_f^{FC}
36 atom cell	450	3.63	3.01	2.79	2.67
	550	3.64	3.02	2.80	2.68
48 atom cell	450	3.65	3.04	2.82	2.69

is 0.29 eV lower than that in octahedral one, qualitatively consistent with the results of earlier work [21–24].

Another noticeable point is that the formation energy of He in substitutional site (E_f^{sub}) is higher than that of He in interstitial site in hcp Ti. This behavior is similar to those of He in bcc V (vanadium) and bcc Nb in Ref. [24]. The formation energy of a Ti vacancy [$E_f(\text{V})$] is derived in terms of Eq. (1), to be 1.92 eV and the E_f^{sub} represents the energy required to form a HeV complex (Here V is a Ti vacancy). Based on the difference between E_f^{sub} and $E_f(\text{V})$, we obtained the formation energy of 1.7 eV for a He atom in a pre-existing vacancy. Therefore, the binding energy of a He atom bonded to a pre-existing vacancy ($E_{\text{He-V}}^b$) is 0.96 eV as calculated by $E_{\text{He-V}}^b = E_f(\text{He}) + E_f(\text{V}) - E_f^{\text{sub}}(\text{He})$. These results suggest that He atom can be trapped easily as an interstitial defect by a pre-existing vacancy, whereas it is difficult to generate a HeV complex in perfect hcp Ti lattice. For instance, for fcc Ni the formation energy of substitutional He is lower by 2.27 eV than the interstitial one [24], and a cluster consisting of five He atoms is needed to drive one Ni atom away from its equilibrium site (simultaneously producing a Ni vacancy) to its nearest-neighboring interstitial site [15]. Therefore, a cluster consisting more He atoms may be required to create such a Ti vacancy as the formation energy of the substitutional He (E_f^{sub}) is higher than that of interstitial He.

Of particular interesting to us is a highly low formation energy of interstitial He in Ti (2.67 eV). This value is lower significantly than those in bcc Fe (4.39 eV [22], 4.49 eV [24], 5.36 eV [12]) or in fcc Ni (4.52 eV [12], 4.50 eV [24]), implying that He atom in Ti has less difficulty to stay in interstitial sites than in Fe or Ni. The migration activation energy of interstitial He atom along (0 0 1) direction is 0.34 eV as derived by the difference of formation energies of octahedral and FC site, which is higher than that for bcc Fe (0.17 eV [12], 0.06 eV [22]) and fcc Ni (0.08 eV [12]). The high migration activation energy may slow down the growth rate of He bubble.

2.2. Mechanism of He locating at the FC site

To understand the reason as to why the most energy favorable site for interstitial He in hcp Ti is FC site, the formation energy of an interstitial He are divided into three parts: the interaction between He atom and its surrounding Ti atoms ($E_{\text{int}}(\text{Ti-He})$), the energy increase induced by the deformation of Ti lattice ($E_{\text{def}}(\text{Ti})$), and the interaction between He atoms ($E_{\text{int}}(\text{He-He})$), that is:

$$E_f = E_{\text{int}}(\text{Ti-He}) + E_{\text{def}}(\text{Ti}) + E_{\text{int}}(\text{He-He}), \quad (2)$$

and

$$E_{\text{int}}(\text{Ti-He}) = E(m\text{Ti}, \text{He}) - E(m\text{Ti})^* - E(\text{He})^*,$$

$$E_{\text{def}}(\text{Ti}) = E(m\text{Ti})^* - mE(\text{Ti}),$$

$$E_{\text{int}}(\text{He-He}) = E(\text{He})^* - E(\text{He}),$$

where $E(m\text{Ti}, \text{He})$ is the total energy of optimized supercell consisting of $m\text{Ti}$ atoms and a He atom; $E(m\text{Ti})^*$ [or $E(\text{He})^*$] is the single point energy of the supercell containing $m\text{Ti}$ atom (or one He atom), with the atom position and cell parameters same as those of $E(m\text{Ti}, \text{He})$. The results of different interstitial He sites are listed in Table 2,

Table 2

The E_f , volume swelling rate (ω), $E_{\text{int}}(\text{Ti-He})$, $E_{\text{int}}(\text{He-He})$, and $E_{\text{def}}(\text{Ti})$ of different interstitial He sites.

	E_f	ω	$E_{\text{int}}(\text{Ti-He})$	$E_{\text{int}}(\text{He-He})$	$E_{\text{def}}(\text{Ti})$
Ti36He (TC)	2.79	0.012	2.21	-0.002	0.59
Ti36He (OC)	3.01	0.013	2.24	0.001	0.77
Ti36He (FC)	2.67	0.012	2.16	0.000	0.51

together with the ratio of volume swelling (ω) induced by dissolution of He atom.

From Table 2, the interaction energy between He atoms is only several parts per thousand of a electron volt, indicating that the He–He interaction is too weak to be considered. For each interstitial configuration, more than 75% of its formation energy is the interaction energy between a He atom and its surrounding Ti atoms $E_{\text{int}}(\text{Ti-He})$, and the rest is the deformation energy $E_{\text{def}}(\text{Ti})$. Both the Ti–He interaction and the deformation energy of Ti in the FC configuration are the lowest among the three ones, which render FC site suitable for interstitial He in Ti. In addition, the volume swelling rates of both FC and TC configurations are the lower than that of OC configuration, as reflected by the deformation energy of Ti lattice.

From the point of view for electronic distribution, according to Refs. [34,35], the solution heat of interstitial He atom in metals is

mainly decided by the interstitial electron densities: the minimum-energy site in perfect crystal is the site with lowest charge density.

Total charge density ($\rho(r)$) of pure Ti crystal has been calculated and its isosurfaces with $\rho(r)$ of 165 and 150 e/nm^3 are illustrated in Fig. 2a and b, respectively. The former is a type of tubes along the $\langle 001 \rangle$ direction, covering the octahedral and the FC sites. As the charge density inside the tube is lower than that of the outside, the interstitial He atoms could more easily stay inside and travel along these tubes than other zones in accordance with the results of molecular dynamic study [36], in which He inter-layer jump (along $[001]$ direction) occurs more frequently than the intra-layer jump [in (001) crystal plane]. Apparently, the tube around octahedral sites shows a larger space than those around FC sites. However, it has been found that the ellipsoid isosurfaces with $\rho(r) = 150 \text{ e}/\text{nm}^3$ in Fig. 2b are centered at FC sites. Therefore, the positions with

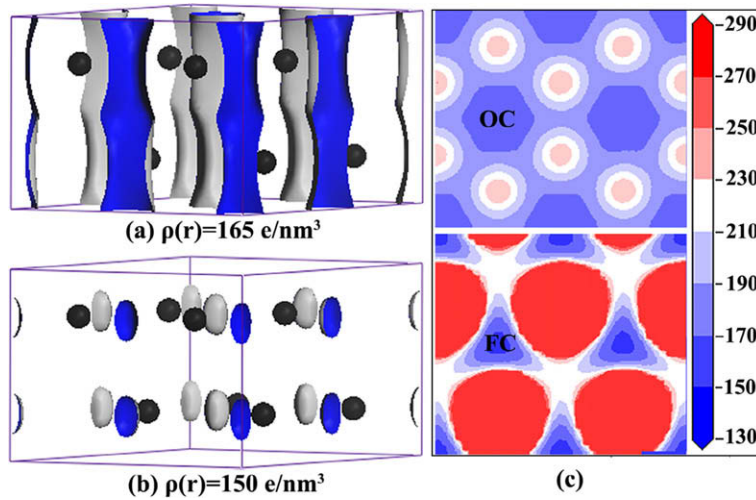


Fig. 2. The charge density ($\rho(r)$) in perfect hcp titanium crystal: (a) and (b) the isosurfaces of $\rho(r) = 165$ and $150 \text{ e}/\text{nm}^3$; (c) the contour plots of the charge density of the (001) planes crossing OC and FC sites. In (a) and (b), the black ball in represents Ti atom, the blue and light grey surface represent the inside and outside of the isosurface. (For interpretation of the references to colour in this figure legend, the reader is referred to the web version of this article.)

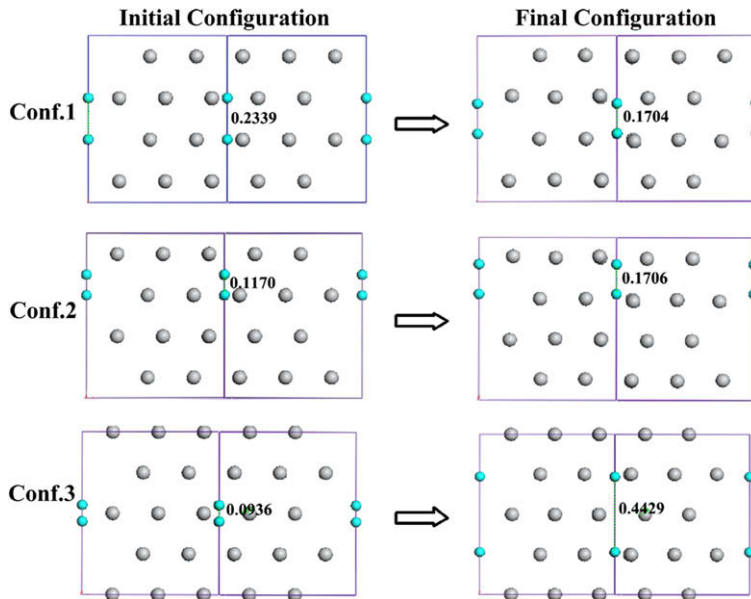


Fig. 3. The three kinds of initial configurations (left panel) of two He atoms in 36-atom Ti supercell and their final optimized configurations (right panel). The grey and light blue balls represent Ti and He atom, respectively. (For interpretation of the references to colour in this figure legend, the reader is referred to the web version of this article.)

the lowest charge density are the FC sites, which can also be explicitly seen from the charge density of the (0 0 1) planes crossing OC and FC sites in Fig. 2c. This feature may be responsible for the lowest formation energy for the interstitial He atom at a smaller-spacer FC site, rather than at a large-spacer OC site.

2.3. Clustering of He atoms

To elaborate the clustering behavior of He atoms in hcp Ti, we further optimized three configurations varying two He atoms in three types of arrays. Given that the FC site is the preferable site for interstitial He atom, each initial configuration is built with at least one He atom at the FC site. The initial and the optimized structures are shown in Fig. 3. As shown in Conf. 1, the two He atoms initially occupy two first-nearest neighbored FC sites separated by a distance of 0.2339 nm. After the relaxation, these two He atoms form a dimer along the $\langle 001 \rangle$ direction centered at the octahedral site, with an average formation energy of 2.34 eV per He atom (derived from $E_{\text{form}}(\text{He}_2)/2$). In the initial configuration of Conf. 2, one He atom occupies a FC site and the second He lies in the first He atom's first-neighbored octahedral site. Although the initial configuration of Conf. 2 is obviously different from that of Conf. 1, it has been proven that both Confs. 1 and 2 are eventually converged to an almost same configuration (c.f., Table 3 and Fig. 3). In Conf. 3 considered here, two He atoms originally locate at two FC site as a dumbbell separated by 0.0936 nm along the $\langle 001 \rangle$ direction. After optimization, they depart from each other and go to the neighbored FC sites separated by 0.4429 nm. From these results above, it can be concluded that two interstitial He atoms tend to agglomerate at the neighborhood of an OC site rather than FC site, although FC site is the most favorable one for an isolated He atom. According to the equation $E_{\text{bind}} = 2E_{\text{int}}(\text{He}) - E_{\text{form}}(\text{He}_2)$, the bind energy of one He atom to another He in Ti is as high as 0.66 eV, suggesting that interstitial He atom in Ti could be easily trapped by another. This situation is comparable to that in bcc Fe where the bonding energy of two He atoms is only 0.43 eV [22]. Considering the binding energy of a He atom to a pre-existing vacancy, 0.96 eV, the comparable bind-

ing ability of two He atoms (0.66 eV) may be responsible for the experimental observation [5]: when the He concentration is only a few tens of appm in α -Ti, the distribution of He bubbles correlated little to grain boundaries and dislocations, which are in the vacancy-rich zones. When the He concentration is high enough to be accommodated by the limited vacancy inside the grain, more He bubbles distribute in grain boundaries and dislocations [9].

2.4. The stability of He_n and He_nV clusters

It is also interesting to see how many He atoms can be stabilized around an interstitial He atom and the substitutional one (HeV complex). The stability of He_n and He_nV clusters are further investigated with $n = 1-6$. Considering the favorable interstitial site is a face-centered position of octahedron in hcp Ti and He_2 cluster is indeed a dimer within octahedron, the configuration for He_n ($n > 2$) is built by putting more He atoms at the face centers of an octahedron, simultaneously keeping high symmetry and short distance between He atoms. He_nV cluster are built in the same way in which all He atoms are around a Ti vacancy. All the configurations are optimized and their formation energies of He_n and He_nV are compiled in Fig. 4a. The formation energy of He_n cluster are lower than that of He_nV cluster, when $n \leq 2$. The trend is reversed when $n \geq 3$: He_nV clusters are more stable than He_n cluster.

In Fig 4b, we observed that average formation energy per He decreases with increasing n in the case of the He_nV cluster and reach a minimum at $n = 5$, indicating an increasingly binding trend for interstitial He added to the He_nV cluster in Titanium. This situation implies that, if a He atom is trapped by a pre-existing Ti vacancy and form a HeV unit, it will attract more interstitial He atoms to form a He_nV cluster. In addition, to ensure whether or not a 36 Ti-atom supercell is large enough to study the behaviors of He_n and He_nV ($n \leq 6$) clusters, the formation energy of He_6 cluster, which induces the largest volume swelling, has been double checked in a 54-atom supercell. The results show that the formation energy of He_6 cluster in the 54-atom supercell is slightly higher by 0.04 eV than that in the 36 Ti atom cell. This comparison suggests that the results for He_n and He_nV ($n \leq 6$) clusters in 36 atom cell are quantitatively reliable.

3. Conclusions

In this paper, we have investigated the behaviors of He in hcp-type Ti through first-principles calculations. For an isolated He atom in Ti, the most favorable interstitial site is a novel interstitial site (called FC site; namely, the center of the face shared by two adjacent octahedrons) with formation energy of 2.67 eV. This can be attributed to the weak interaction between He atom in the FC

Table 3
The He–He distances in initial and optimized configurations, $D_{(\text{He}-\text{He})}^{\text{init}}$ and $D_{(\text{He}-\text{He})}^{\text{opt}}$, as well as the formation energy of He dimer, $E_f(\text{He}_2)$, in 36-atom supercell of Ti.

	$D_{(\text{He}-\text{He})}^{\text{init}}$ (nm)	$D_{(\text{He}-\text{He})}^{\text{opt}}$ (nm)	$E_{\text{form}}(\text{He}_2)$ (eV)
Conf. 1	0.2339	0.1704	4.69
Conf. 2	0.1170	0.1706	4.68
Conf. 3	0.0936	0.4429	5.44

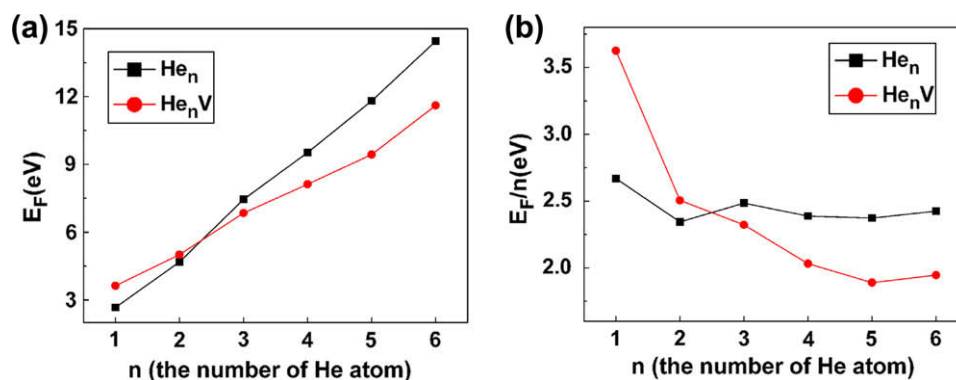


Fig. 4. Formation energy of He_n and He_nV clusters as a function of with the number of He in clusters, n ; panel (a), the total formation energy and panel (b) average formation energy per He atom.

site and its surrounding Ti atoms mainly due to the lowest charge density at the FC site of defect-free hcp Ti lattice. The fact that the formation energy of interstitial He is lower than that of substitutional one suggests that interstitial He atom is difficult to substitute a Ti atom in perfect hcp Ti lattice to form a HeV cluster. However, we found that He can easily be trapped by a pre-existing vacancy with a binding energy of 0.96 eV. In addition, an interstitial He atom can be easily trapped by another He atom with a binding energy as high as 0.66 eV and form a dimer centered at the octahedral site via migrating easily along $\langle 001 \rangle$ direction with an activation energy of 0.34 eV. Furthermore, we also investigated the behavior of He_nV clusters and found that they are more stable than He_n clusters with $n \geq 3$. The decreasing of average formation energy per He for He_nV cluster with $n \leq 5$ possibly suggests the enhanced growth of He bubbles with Ti vacancy.

References

- [1] L.C. Beavis, C.J. Miglionico, *J. Less-Common Met.* 27 (1972) 201.
- [2] G.J. Thomas, J.M. Mintz, *J. Nucl. Mater.* 116 (1983) 336.
- [3] T. Schober, R. Lasser, *J. Nucl. Mater.* 120 (1984) 137.
- [4] T. Schober, R. Lasser, J. Golczewski, et al., *Phys. Rev. B* 31 (1985) 7109.
- [5] T. Schober, K. Farrell, *J. Nucl. Mater.* 168 (1989) 171.
- [6] G.C. Abell, L.K. Matson, R.H. Steinmeyer, et al., *Phys. Rev. B* 41 (1990) 1220.
- [7] G.C. Abell, D.F. Cowgill, *Phys. Rev. B* 44 (1991) 4178.
- [8] S. Thiebaut, B. Decamps, J.M. Penisson, et al., *J. Nucl. Mater.* 277 (2000) 217.
- [9] H. Zheng, S. Liu, H.B. Yu, et al., *Mater. Lett.* 59 (2005) 1071.
- [10] R.C. Bowman, A. Attalla, *Phys. Rev. B* 16 (1977) 1828.
- [11] W.D. Wilson, C.L. Bisson, *Phys. Rev. B* 3 (1971) 3984.
- [12] W.D. Wilson, R.A. Johnson, in: P.C. Gehlen, J.R. Beeler, R.I. Jaffee (Eds.), *Interatomic Potentials und Simulation of Lattice Defects*, Plenum Press, New York, 1972, p. 375.
- [13] W.D. Wilson, M.I. Baskes, C.L. Bisson, *Phys. Rev. B* 13 (1976) 2470.
- [14] W.D. Wilson, in: F.W. Young, M.T. Robinson (Eds.), *Conference on Fundamental Aspects of Radiation Damage in Metals*, National Technical Information Service, Springfield, VA Report No. USERDA-CONF-751006-P2 1979, p. 1025.
- [15] W.D. Wilson, C.L. Bisson, M.I. Baskes, *Phys. Rev. B* 24 (1981) 5616.
- [16] B.B. Nielsen, A.V. Veen, *J. Phys. F: Met. Phys.* 15 (1985) 2409.
- [17] K.O. Jensen, R.M. Nieminen, *Phys. Rev. B* 35 (1987) 2087.
- [18] G.J. Ackland, D.J. Bacon, A.F. Calder, T. Harry, *Philos. Mag. A* 75 (1997) 713.
- [19] B.J. Lee, M.I. Baskes, H. Kim, Y.K. Cho, *Phys. Rev. B* 64 (2001) 184102.
- [20] L. Wang, X.J. Ning, *J. Phys. Soc. Jpn.* 73 (2004) 943.
- [21] C. Domain, C.S. Becquart, *Phys. Rev. B* 65 (2002) 024103.
- [22] C.C. Fu, F. Willaime, *Phys. Rev. B* 72 (2005) 064117.
- [23] T. Seletskaya, Y. Osetsky, R.E. Stoller, et al., *Phys. Rev. Lett.* 94 (2005) 046403.
- [24] L. Yang, X.T. Zu, X.Y. Wang, et al., *J. Univ. Electron. Sci. Technol. China* 37 (4) (2008) 558 (in Chinese).
- [25] C.S. Becquart, C. Domain, *Phys. Rev. Lett.* 97 (2006) 196402.
- [26] R.P. Gupta, M. Gupta, *Phys. Rev. B* 66 (2002) 014105.
- [27] X.X. Ma, J.L. Li, M.R. Sun, *Appl. Surf. Sci.* 254 (2008) 6837.
- [28] K.L. Shanahan, J.S. Holder, *J. Alloys Compd.* 446–447 (2007) 670.
- [29] L.Q. Shi, C.Z. Liu, S.L. Xu, Y.Z. Zhu, *Thin Solid Films* 479 (2005) 52.
- [30] A.I. Vedenev, V.N. Lobanov, S.V. Starovoitova, *J. Nucl. Mater.* 233–237 (1996) 1189.
- [31] D. Vanderbilt, *Phys. Rev. B* 41 (1990) 7892.
- [32] J.P. Perdew, J.A. Chevary, S.H. Vosko, K.A. Jackson, M.R. Pederson, D.J. Singh, C. Fiolhais, *Phys. Rev. B* 46 (1992) 6671.
- [33] B.G. Pfrommer, M. Cote, S.G. Louie, M.L. Cohen, *J. Comput. Phys.* 131 (1997) 133–140.
- [34] J.K. Norskov, *Phys. Rev. B* 26 (1982) 6.
- [35] J.K. Norskov, F. Besenbacher, J. Bottiger, B.B. Nielsen, A.A. Posarev, *Phys. Rev. Lett.* 49 (1982) 1420.
- [36] M. Chen, Q. Hou, J. Wang, T.Y. Sun, X.G. Long, S.Z. Luo, *Solid State Commun.* 148 (2008) 178.